

Matter near to the Endpoint of the Electroweak Phase Transition

E.-M. Ilgenfritz^a, A. Schiller^{b*} and C. Strecha^b^aInstitute for Theoretical Physics, Kanazawa University, Kanazawa 920-1192, Japan^bInstitut für Theoretische Physik and NTZ, Universität Leipzig, D-04109 Leipzig, Germany

Wave functions and the screening mass spectrum in the 3D $SU(2)$ -Higgs model near to the phase transition line below the endpoint and in the crossover region are calculated. In the crossover region the changing spectrum versus temperature is examined showing the aftermath of the phase transition at lower Higgs mass. Large sets of operators with various extensions are used allowing to identify wave functions in position space.

According to recent lattice studies in 3D [1] and 4D [2] the $SU(2)$ -Higgs model ceases to possess a first order transition for a Higgs mass $M_H > 72$ GeV. This and the small amount of CP violation in the standard model seem to rule out the possibility to explain the BAU generation within the standard model.

The lattice version of the $SU(2)$ -Higgs model is still interesting as a laboratory for investigating the behaviour of hot gauge fields coupled to scalar matter, for the characterisation of possible bound states, for the understanding of real time topological transitions and the role of embedded topological defects [3] at the transition.

The 3D lattice model is defined by the action

$$S = \beta_G \sum_p \left(1 - \frac{1}{2} \text{tr} U_p\right) - \beta_H \sum_{x,\mu} S_{x,\mu}(1) + \sum_x (\rho_x^2 + \beta_R (\rho_x^2 - 1)^2). \quad (1)$$

The lattice couplings are related to the continuum parameters of the 3D $SU(2)$ -Higgs model g_3 , λ_3 and m_3 (see *e.g.* [4])

$$\beta_G = \frac{4}{ag_3^2}, \quad \beta_H = \frac{2(1 - 2\beta_R)}{6 + a^2 m_3^2},$$

$$\beta_R = \frac{\lambda_3 \beta_H^2}{g_3^2 \beta_G} = \frac{1}{8} \left(\frac{M_H^*}{80 \text{ GeV}} \right)^2 \frac{\beta_H^2}{\beta_G}, \quad (2)$$

they can be expressed via perturbation theory in terms of 4D couplings and masses [5]. The parameter M_H^* is approximately equal to the zero

*Talk at LAT'98 given by A. Schiller

temperature physical Higgs mass. The summation in (1) is taken over plaquettes p , sites x and links $l = \{x, \mu\}$. The gauge fields are represented by unitary 2×2 link matrices $U_{x,\mu}$, U_p denotes the $SU(2)$ plaquette matrix. The Higgs field is parametrised as follows: $\Phi_x = \rho_x V_x$ with $\rho_x^2 = \frac{1}{2} \text{tr}(\Phi_x^\dagger \Phi_x)$ and V_x is an element of the group $SU(2)$, $S_{x,\mu}(1)$ is defined below in (4).

Here we report on some results of our recent study [6] of the screening spectrum across the very weak phase transition ($M_H^* = 70$ GeV) and the crossover region (at $M_H^* = 100$ GeV). This complements earlier studies near to a strongly first order transition and at markedly larger Higgs mass [7]. Details of the update algorithms have been reported before [4].

To study simultaneously the ground state and excited states (as well as their wave functions) one has to consider cross correlations between (time-slice sums of) operators \mathcal{O}_i from a complete set in a given J^{PC} channel with quantum numbers J (angular momentum), P (parity) and C (charge conjugation). According to the transfer matrix formalism, one should be able to write the connected correlation matrix at time separation t in the spectral decomposition form $C_{ij}(t) = \sum_{n=1}^{\infty} \Psi_i^{(n)} \Psi_j^{(n)*} e^{-m_n t}$ with $\Psi_i^{(n)} = \langle \text{vac} | \mathcal{O}_i | \Psi^{(n)} \rangle$, $|\Psi^{(n)}\rangle$ is the n -th (zero momentum) energy eigenstate. By suitable diagonalisation this allows to find masses and wave functions of the lowest mass screening states (ground state) and higher mass excited states in the various J^{PC}

channels. However, in practice one has to choose a truncated set of operators \mathcal{O}_i , ($i = 1, \dots, N$).

Solving the generalised eigenvalue problem $C(t)\Psi^{(n)} = \lambda^{(n)}(t, t_0)C(t_0)\Psi^{(n)}$ or $\tilde{C}(t, t_0)\tilde{\Psi}^{(n)} = \lambda^{(n)}(t, t_0)\tilde{\Psi}^{(n)}$, with $\tilde{C}(t, t_0) = C^{-\frac{1}{2}}(t_0)C(t)C^{-\frac{1}{2}}(t_0)$ ($t > t_0$, where $t_0 = 0, 1, 2$), errors related to this truncation can be kept minimal [8]. Practically the decomposition of the matrix $C(t_0)$ is performed using a Cholesky decomposition: $C(t_0) = LL^T$. The optimised eigenfunctions $\Psi^{(n)}$ in the chosen operator basis (obtained with a small distance t_0) give an information about the overlap of the source operators \mathcal{O}_i with the actual eigenstates $|\Psi^{(n)}\rangle$. The masses $m^{(n)}$ of these states are obtained by fitting the diagonal elements $\mu^{(n)}(t, t_0) = \tilde{\Psi}^{(n)}\tilde{C}(t, t_0)\tilde{\Psi}^{(n)}$ to a hyperbolic cosine form with t in some plateau region of a local effective mass.

In contrast to a smearing technique for gauge links and Higgs fields [7], we have collected only a few types of operators \mathcal{O}_i in our base but with a wide span of sizes l in lattice spacings. Such a basis allows to obtain information on the spatial extension of a bound state without going through a variational procedure. Here, we have restricted ourselves to the following operators (with $\mu = 3$ reserved for the correlation direction):

$$0^{++} : \rho_x^2, S_{x,1}(l) + S_{x,2}(l), W_{x,1,2}(l) + W_{x,2,1}(l) \\ 1^{--} : V_{x,1}^b(l) + V_{x,2}^b(l), 2^{++} : S_{x,1}(l) - S_{x,2}(l) \quad (3)$$

where

$$S_{x,\mu}(l) = \frac{1}{2}\text{tr}(\Phi_x^+ U_{x,\mu} \dots U_{x+(l-1)\hat{\mu},\mu} \Phi_{x+l\hat{\mu}}), \quad (4)$$

$$V_{x,\mu}^b(l) = \frac{1}{2}\text{tr}(\tau^b \Phi_x^+ U_{x,\mu} \dots U_{x+(l-1)\hat{\mu},\mu} \Phi_{x+l\hat{\mu}}),$$

$W_{x,\mu,\nu}(l)$ are quadratic Wilson loops of size $l \times l$.

Using the cross correlation technique we were able to obtain the wave function squared corresponding to the optimised operator for each individual state in the spectrum. Being functions of a physical distance, the squared wave functions are shown immediately *vs. lag*₃² in order to overlay data from measurements at various gauge couplings (lattice spacings) taken along a line of constant physics near to the transition temperature.

Results for the 0^{++} channel are collected in Figs. 1-3 for the squared wave functions. The

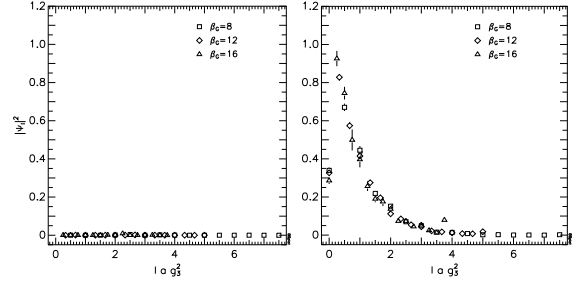


Figure 1. Squared wave function of the ground state in the 0^{++} channel, measured on a 30^3 lattice in the symmetric phase; left: $W_{x,1,2}(l) + W_{x,2,1}(l)$, right: $S_{x,1}(l) + S_{x,2}(l)$; $l = 0, \dots, 15$

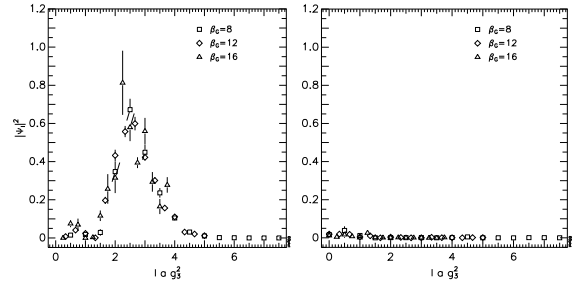


Figure 2. Same as Fig. 1 for the second excited state

contributions from the Higgs string and Wilson loop operators are shown separately in order to identify clearly Higgs and W -ball excitations. In the symmetric phase we observe no mixing of these two operator types in the Higgs ground state and the first excitation (not shown). The second excited state consists of a pure excitation of gauge degrees of freedom (d.o.f.) and can be identified with a W -ball in analogy with the glueballs of pure $SU(2)$. Our results on this decoupling confirm the observations in [7] made at a much lighter Higgs mass.

On the Higgs side of the phase transition pure gauge matter (W -ball) excitations are not expected to be present in the spectrum. In the 0^{++} channel, our operator set is sufficient to observe a marked difference between the phases which is not in accordance to naive expectations. We observe a mixing between the two operator types, W -ball operators (pure gauge d.o.f.) and operators projecting onto Higgs states. This is demonstrated for the first excited Higgs state which contains a noticeable contribution from Wilson loop operators (Fig. 3). We interpret this mixing of Higgs and gauge d.o.f. as a signal of the near endpoint

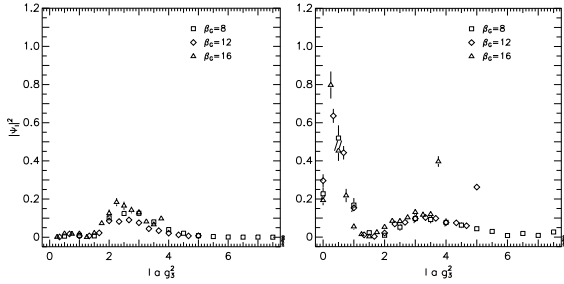


Figure 3. Same as Fig. 1 for the first excited state in the Higgs phase

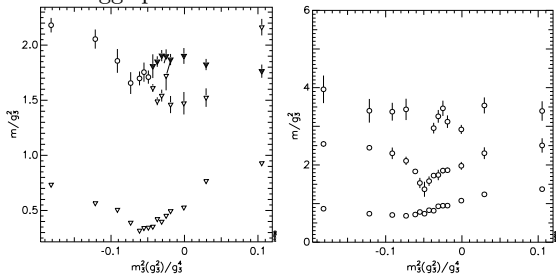


Figure 4. Screening mass spectra near the crossover in channels 0^{++} and 1^{--} ; 0^{++} : (∇) Higgs states, (full triangles) W -ball states (\circ) Higgs states with an admixture of excited gauge d.o.f.

of the phase transition. Deeper in the Higgs phase the contribution from gauge d.o.f. is expected to disappear which has been checked in our simulations at $M_H^* = 100$ GeV.

The spectrum change has been studied in more detail at $M_H^* = 100$ GeV while *continuously* passing the crossover line (changing β_H) at fixed gauge coupling $\beta_G = 12$. We have found a behaviour very similar to our results obtained at $M_H^* = 70$ GeV. The similarities concern both the high temperature side of the crossover (where one expects thermodynamic properties being close to those of the symmetric phase at smaller Higgs mass) and the region very near to the crossover line on the so-called Higgs side of the crossover.

In Fig. 4 we present the spectrum of the lowest states in the 0^{++} and 1^{--} channels as function of $m_3^2(g_3^2)/g_3^4$ (or β_H) over a certain interval above and below the crossover (*i.e.* in temperature). Looking at the excited states in the 0^{++} channel of Figs. 4 we conclude that the scalar and gauge sector are approximately decoupled as long as one keeps away from the crossover line on the high temperature side. The mass of the lowest W -ball state (full triangle) is roughly independent of β_H

as long as one does not come too close to the crossover. Thus, on the high temperature side of the crossover, the ordering of states qualitatively resembles the spectrum at smaller values of Higgs self-coupling (at $M_H^* = 70$ GeV).

If one approaches the crossover temperature the mass of the first (Higgs-like) excitation is moving up towards the lowest W -ball state whose mass decreases. At some point we observe a growing admixture to the Higgs excitation by contributions from Wilson loop operators. We have explicitly checked that at higher β_H (deeper in the would-be Higgs phase) the admixture from pure gauge d.o.f. disappears again from this state.

To summarise, our operator choice was the simplest one to incorporate the notion of spatial extension. The continuum limit of the screening masses and wave functions has to be accompanied by correspondingly larger lattices with the same physical volume, without automatically enlarged operator basis. Therefore, in a next step of improvement of the method, smearing of the fields entering our operators and/or the construction of blocked operators will become necessary for further optimising the resolving capability of the method for excited states.

REFERENCES

1. K. Kajantie et al., Phys. Rev. Lett. 77 (1996) 2887; F. Karsch et al., Nucl. Phys. (Proc. Suppl.) 53 (1997) 623; M. Gürtler, E.-M. Ilgenfritz, and A. Schiller, Phys. Rev. D56 (1997) 3888.
2. Talks of Y. Aoki and Z. Fodor, these proceedings
3. M. N. Chernodub et al., hep-lat/9805016, to appear in Phys. Lett. B; hep-lat/9807016.
4. M. Gürtler et al., Nucl. Phys. B483 (1997) 383.
5. K. Kajantie et al., Nucl. Phys. B458 (1996) 90.
6. E.-M. Ilgenfritz, A. Schiller and C. Strecha, hep-lat/9807023.
7. O. Philipsen, M. Teper, and H. Wittig, Nucl. Phys. B469 (1996) 445; hep-lat/9709145, to appear in Nucl. Phys. B.
8. M. Lüscher and U. Wolff, Nucl. Phys. B339 (1990) 222; C. R. Gatttringer and C. B. Lang, Nucl. Phys. B391 (1993) 463.